Low-temperature characterization of bitumen and correlation to chemical properties

Kristina Hofer [a],[*], Johannes Mirwald [a], Amit Bhasin [b], Bernhard Hofko [a]

[a] *Christian Doppler Laboratory for Chemo-Mechanical Analysis of Bituminous Materials, Institute of Transportation, TU Wien, Vienna, Austria*
[b] *Department of Civil, Architectural and Environmental Engineering, The University of Texas at Austin, Austin, TX, USA*

ABSTRACT

A comprehensive understanding of the low-temperature performance of bitumen presents a crucial aspect in the durability of asphalt pavements. In order to capture these properties, current low-temperature testing by the bending beam rheometer (BBR) requires a relatively high amount of aged material, which is not always available. In recent studies, the complex shear modulus and phase angle acquired using a 4 mm geometry with the dynamic shear rheometer (DSR) have been used directly as a criterion for the lower performance grade of bitumen. The purpose of the presented study was to assess the application of the previously developed 4 mm DSR test method for material characterization at low temperatures and to develop a correlation between mechanical and chemical properties. BBR and DSR measurements were performed on 8 non-modified and 4 polymer-modified binders. Fourier transform infrared (FTIR) spectroscopy and SARA fractionation were used to gather chemical information about the samples. A strong linear correlation ($R^2 = 0.93$) between the results from BBR and DSR measurements could be observed, allowing an accurate assignment of the low-temperature performance grade for a majority of the investigated samples. Additionally, connections between the FTIR aging index, asphaltene content and the ratio of SARA fractions to the continuous lower performance grade and ΔT_c were observed. This demonstrates the potential of chemical analysis methods to provide information about the low-temperature properties of bitumen.

1. Introduction

Due to contact with reactive oxygen species (ROS) and various other environmental factors, bituminous binders undergo oxidation during their life span. This leads to an increase in stiffness and viscosity along with a decreased ability to dissipate stresses due to viscoelastic relaxation [1,2]. Hence, the occurrence of aging is one of the main causes for the cracking of asphalt pavements at lower temperatures and therefore premature material failure [3–5]. For the low-temperature assessment of bitumen in the laboratory, several methods have been developed, whereby the bending beam rheometer (BBR) is one of the most commonly applied devices [6]. The major disadvantage of this method is the relatively large amount of material needed for one test. This is especially challenging when handling reclaimed asphalt pavement (RAP) or emulsion residue, as there is usually only a limited amount of material available. The recycling of asphalt and thus, the accurate characterization of the reclaimed material is of crucial importance in ensuring a high-quality product for application, while moving into an environmentally friendly and sustainable circular economy in transport infrastructure.

Thus, the development of an alternative low-temperature characterization method for bitumen has been focused on increasingly over the last decade. The dynamic shear rheometer (DSR) has been used successfully for the measurement of material properties in the high and intermediate temperature range, whereby only approximately 1 g of sample is necessary. In the past, low-temperature measurements of bituminous binders with the DSR were not possible due to the high material stiffness, limited torque and insufficient temperature conditioning of the test equipment. However, thanks to the improvement and evolution of DSR devices these shortcomings lie in the past. Sui et al. [7] developed a new technique for measuring low-temperature properties of bitumen by using 4 mm-parallel plates on a DSR, requiring only about 25 mg of material instead of 15 g for BBR measurements. Thereby, an important parameter that has to be considered is the machine compliance. Two different methods for machine compliance correction were applied, firstly the previously collected data was corrected using a mathematical equation and secondly an automatic correction with a pre-input machine compliance was performed.

* Corresponding author.
  E-mail address: kristina.hofer@tuwien.ac.at (K. Hofer).

Consistency between both compliance correction methods was proved and the results showed good reliability and repeatability. Based on this research, the analysis method was further developed by investigating various approaches for machine compliance [8], thermal and mechanical equilibrium, different types of sweep tests and also repeatability when being performed by different testing personnel and laboratories [9–11]. Furthermore, the possibility to use the DSR for low-temperature grading of bitumen and thereby the correlation to other test methods, e.g. the BBR [8], was proposed. Possible correlation parameters between the two measurements devices were investigated, whereby van Heerden et al. [12] proposed a connection between BBR creep stiffness and DSR shear stress relaxation data and Lu et al. [13] found certain statistical correlations when looking at BBR stiffness versus DSR complex modulus and m-value versus phase angle. Furthermore, studies with polymer-modified binder samples were performed, where a linear correlation between the BBR flexural creep stiffness and the DSR complex modulus could be observed. Deviations from this trend were explained by macro-phase separation between the respective polymer and the binder due to the poor compatibility of the two materials [14]. The observed link between the two devices has laid the foundation for a possible low-temperature performance grading (PG) criterion based on DSR instead of BBR measurements. For that, several different approaches were developed, which in general were based on the idea of correlating and converting DSR to BBR data. Therefore, a conversion of the DSR measurements from shear to flexural data and from frequency to time domain is necessary. For this transformation the Christensen Anderson and Marasteanu (CAM) or the Maxwell model were used in many cases followed by a certain definition of a stiffness grading criterion [8,13,15–18]. With these mathematical transformations it is possible to correlate DSR to BBR measurements, whereby the overall accuracy depends on the respective analysis and model. However, the requirement of applying mathematical interconversions on the data entails two major drawbacks: Firstly, the comparison of results gathered via different models and calculations is rather challenging and secondly the applicability of the method for routine testing is limited. Therefore, Komaragiri et al. [19] evaluated a different approach using the DSR complex modulus and phase angle directly for the determination of the low-temperature PG without any mathematical conversion. In a first step the linear correlation between DSR and BBR data was determined, followed by the definition of cut-off values for the complex modulus and the phase angle. These values can then be used in lieu of the respective values for the stiffness and m-value. With this approach it was possible to characterize the low-temperature behavior of a diverse and large test set of bitumens in a simple and quick manner.

Another important parameter for the characterization of bitumen is the difference in the low-temperature PG limiting temperatures ΔT_c. It gives information about relaxation properties and therefore about age-related embrittlement and durability properties of the investigated material. The determination of ΔT_c can be performed according to Equation (1), whereby $T_{c,S(60s)}$ represents the continuous limiting temperature for the creep stiffness S and $T_{c,m(60s)}$ for the creep rate m-value. Both values can be obtained during standard BBR measurements.

$$\Delta T_c = T_{c,S(60s)} - T_{c,m(60s)} \tag{1}$$

The sign of ΔT_c is an indication whether the low-temperature properties of the respective binder are essentially influenced by the stiffness S or the creep rate m-value. If the investigated material fails the S-criterion first, ΔT_c shows a positive value and the material is S-controlled. Inversely, ΔT_c shows a negative value and the material is m-controlled. In general it was observed, that aging and/or the addition of RAP resulted in an increasingly negative value for ΔT_c [20,21]. Additionally, highly negative values are suspected to be correlated to fatigue cracking or other failure behaviors induced by impaired relaxation properties [22]. In order to explain the mechanical response of the material in the low-temperature domain also a link to its chemical composition needs to be established.

The purpose of the present study was to gain insight on the mechanical low-temperature behavior of various bituminous binders and to establish a correlation to changes in the chemical composition. Therefore, BBR and DSR measurements of 8 non-modified and 4 polymer-modified bitumen were conducted between –30 and –6 °C following the test method proposed in [19]. Thereby, the lower PG based on both DSR and BBR measurements and the difference in the low PG limiting temperatures ΔT_c based on BBR measurements were used as assessment parameters. Furthermore, FTIR spectroscopy and SARA fractionation with solid phase extraction (SPE) cartridges were used to gather information about the changes in the chemical composition and in the polarity gradient of the respective binder sample. By combining and correlating the different mechanical and chemical analysis methods, possible links can be determined and a better understanding about the low-temperature performance of bitumen can be obtained.

2. Materials & methods

2.1. Materials

For this study 8 non-modified ("N") and 4 polymer-modified ("P") bitumen were used. As a modifier styrene–butadienestyrene (SBS) was used for all four polymer-modified binders. Their basic properties are summarized in Table 1. For analysis, the materials were measured in an unaged and in a long-term aged (LTA) state. The Rolling Thin Film Oven Test (RTFOT) according to ASTM D2872 – 21 [23] was used for short-term aging (STA) and the Pressure Aging Vessel (PAV) at 100 °C according to ASTM D6521 – 19a [24] was subsequently used for LTA.

2.2. Methods

2.2.1. Bending beam rheometer (BBR)

A COESFELD petrotest bending beam rheometer with a Huber ministate 240 kryostat was used for the low-temperature characterization according to ASTM D6648 – 08 (2016) [25]. For each temperature (–12, –18, −24 and −30 °C) and bitumen two samples were measured.

2.2.2. Dynamic shear rheometer (DSR)

The low-temperature DSR measurements were conducted with an MCR 302 Anton Paar DSR device. For each experiment 1 g of the material was heated up in a metal spoon (up to 120 °C for the unmodified and up to 185 °C for the polymer-modified bitumens), poured into a 4 mm silicone mold and stored in the dark. After 24 ± 2 h the 4 mm plates were preheated to 70 °C, the sample was attached to the upper plate and the gap between the plates was reduced to 2.2 mm. After that the temperature was set to 15 °C, the sample was trimmed and the measurement was conducted using the following frequencies and temperatures:

- 0.03183, 0.1, 0.3, 1, 1.592, 3, 5 Hz
- 0, −6, −12, −18, −24, −30 °C

Table 1
Properties of binders used for study.

Binder	Performance grade (°C)	Needle penetration (1/10 mm)	Softening point (°C)
N.1	58–28	84	45.8
N.2	64–28	62	49.6
N.3	58–28	77	50.8
N.4	64–28	73	55.6
N.5	46–34	168	38.4
N.6	46–28	166	40.2
N.7	52–34	179	37.2
N.8	52–34	171	40.2
P.1	82–28	48	83.5
P.2	82–28	33	82.5
P.3	82–28	52	79.4
P.4	82–28	54	89.5

For the present work, the complex shear modulus $|G^*|$ and the phase angle at 0.03183 Hz were mainly used for further analysis. A high degree of correlation to BBR measurements was observed at this frequency by Komaragiri et al. in a recent study [19].

2.2.3. Attenuated total reflection Fourier-Transformation infrared (ATR-FTIR) spectroscopy

FTIR spectroscopy was used to obtain information about the chemical composition in regards to functional groups present within the respective binder samples. For sample preparation approximately 1 g of the material was collected with a preheated metal spoon and carefully heated with a heat gun. A rod thermometer was used for stirring to ensure proper homogenization and temperature control. After keeping the material at the desired temperature for about 5 min (at 120 °C for the unmodified and at 185 °C for the polymer-modified bitumen) 4 small droplets were placed upon a silicon foil. They were covered immediately with a lid for protection against dust and light-induced aging on the binder surface and measured within 30 min. The sample preparation was performed following general recommendations from Mirwald et al. [26] for handling bitumen prior to FTIR spectroscopy. For the measurement a Bruker Alpha II with a Deuterated Triglycine Sulphate (DTGS) detector and an attenuated total reflection (ATR) unit containing a diamond crystal was used. For each spectrum 24 scans were recorded (at a resolution of 4 cm^{-1}) and four spectra in the range of 4000 – 400 cm^{-1} were measured per droplet, resulting in 16 spectra for each bitumen. Between measurements, the ATR crystal was cleaned with limonene and isopropanol and a background spectrum was recorded. For spectra evaluation and processing the software OPUS was used. A normalization between 3200 and 2800 cm^{-1} and a full base line integration using the following frequency limits was carried out:

- Carbonyls (AI_{CO}): 1800 – 1660 cm^{-1}
- Sulfoxides (AI_{SO}): 1079 – 984 cm^{-1}
- Reference aliphatic band (AI_{CH3}): 1525 – 1350 cm^{-1}

By calculating the Aging Index (AI_{FTIR}) according to Equation (2) (mean value of the respective 16 spectra), the amount of formed carbonyls and sulfoxides and therefore the amount of incorporated oxygen can be assessed for each binder sample.

$$AI_{FTIR} = \frac{(AI_{CO} + AI_{SO})}{AI_{CH_3}} \qquad (2)$$

2.2.4. SARA fractionation with solid phase extraction (SPE) cartridges

For the polarity based separation of the bitumen a simplified procedure developed by Sakib et al. [27] was used. In Fig. 1 an overview of the setup is shown. The fractionation was performed according to the following steps:

1. 400 ± 20 mg of bitumen was put into a glass container with 40 ml of *n*-heptane and stirred with a magnetic stirrer for 24 ± 2 h.
2. Four syringes were each filled with 10 ml of the maltene/asphaltene-mixture and Thermo Scientific™ Titan3™ PTFE syringe filters (25 mm diameter, 0.2 μm pore size) were used to separate the undissolved asphaltenes from the maltene solution. To accelerate the process, the solution was gently pulled through the filter using a vacuum pump and then collected in a glass vial. Once the syringes were empty, the process was repeated with 5 ml of *n*-heptane to dissolve the residual maltene solution.
3. Two of the maltene solutions were dried at ~ 120 °C under a constant N$_2$ stream to prevent aging by atmospheric oxygen. The residue was weighed and the two remaining solutions were diluted with *n*-heptane to ensure a maltene concentration of 3.33 mg/ml.
4. In the next step, the two diluted maltene solutions were separated using a Thermo Scientific™ HyperSep™ Silica SPE cartridge (pore size 40–63 μm). After a pre-wash of the cartridge with 20 ml of *n*-heptane 15 ml of the diluted maltene solution was applied. For the fractionation into saturates, aromatics and resins different solvents were introduced to the cartridge to elute the respective fraction:
   (a) Saturates: 10 ml of *n*-heptane
   (b) Aromatics: 25 ml of 80 % toluene – 20 % *n*-heptane
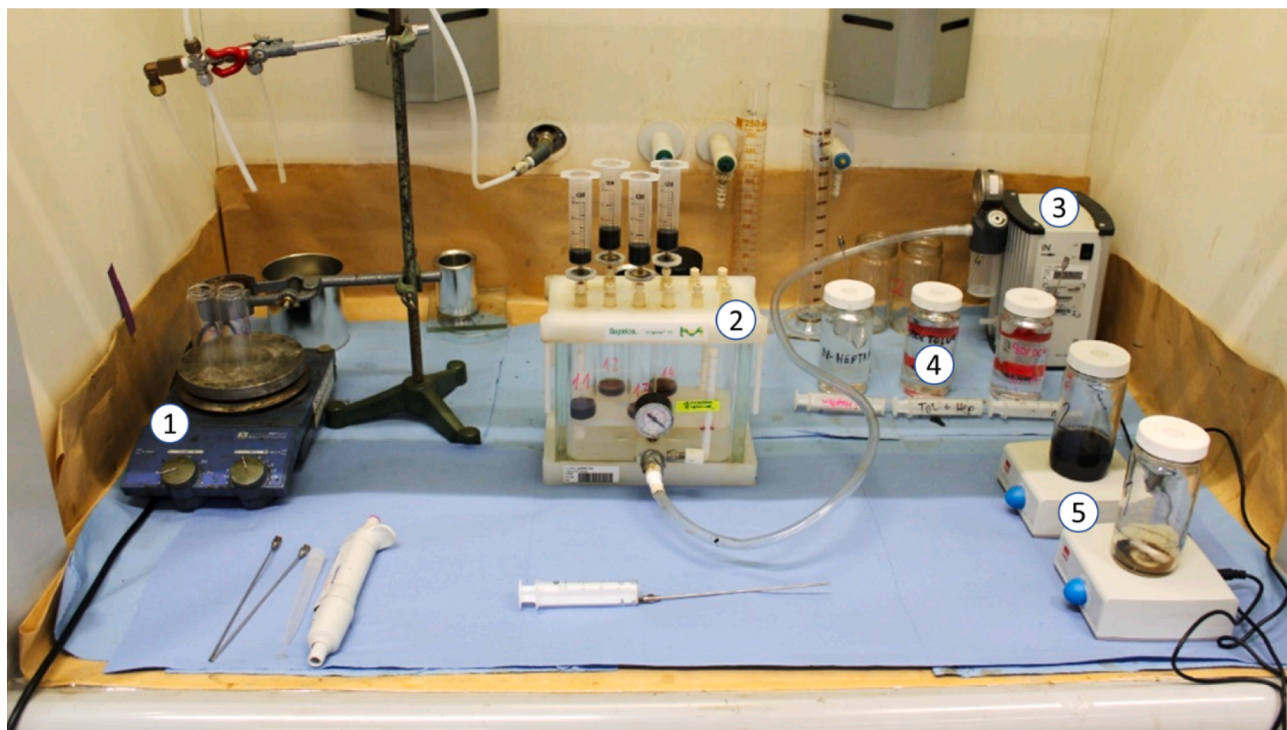   (c) Resins: 40 ml of 90 % dichloromethane – 10 % methanol

Fig. 1. Overview of setup for SARA fractionation; 1) Heating plate and N$_2$ supply for drying, 2) vacuum Manifold with syringes and PTFE syringe filter, 3) vacuum pump, 4) various solvents and 5) glass container with magnetic stirrer.

As in step 2 a vacuum pump was used to gently pull the liquid through the cartridge and the solutions were collected in glass vials.

5. The obtained solutions were then dried as described in step 3. The mass of each fraction was gravimetrically determined and noted. Each separation was repeated 3–4 times per binder.

A summary of all the performed aging and analysis methods can be found in Fig. 2. The aging methods are depicted in grey and the analysis methods in pale pink.

3. Results and discussion

3.1. Correlation between BBR and DSR results

BBR and DSR measurements at −12, −18, −24 and −30 °C were conducted to investigate the correlation between results from both devices. For the results shown below, the BBR stiffness S and m-value were determined after a load duration of 60 s and the DSR complex modulus |G*| and phase angle δ at a frequency of 0.03183 Hz.

In Fig. 3a and Fig. 3b the correlation between the BBR and DSR results at all four temperatures can be seen. Based on general properties, the investigated samples have been divided into three groups, which are represented by different colors and symbols: Binder N.1 to N.4 are described as group "hard" in green with filled symbols, binder N.5 to N.8

as group "soft" in red with half-filled symbols and the polymer-modified binders P.1 to P.4 in blue with empty symbols. In Fig. 3a the BBR S is plotted on the x-axis and the DSR |G*| is plotted on the y-axis. The two parameters show a strong linear dependency with a coefficient of determination of 0.9041. All three binder groups follow this trend, whereby a slight division is visible with increasing S and |G*| at lower temperatures. In Fig. 3b an even more distinct linear correlation with a coefficient of determination of 0.9479 can be observed, when plotting the BBR m-value on the x-axis against the DSR δ on the y-axis. This is also visually underlined by the fact, that there is no division of the binder groups or significant scattering of the data points in the graph. Based on these results, a strong linear correlation between the investigated measurement parameters can be determined. An increase in the stiffness S and m-value measured with the BBR is reflected by an increase in complex modulus |G*| and phase angle δ measured with the DSR. This proves the general link between results from these two measurement devices and the possibility of interchanging one with the other.

It is possible that the test temperature influences the correlation between the two measurement devices. Therefore, DSR |G*| and BBR S have been plotted separately for −12, −18, −24 and −30 °C (see Fig. 4) to assess the relationship at different test temperatures. In Fig. 4a, it can be seen that at −12 °C all the obtained values are in close proximity to each other, with the greatest difference between the results being only 145 MPa for |G*| and 80 MPa for S. This suggests that at −12 °C the
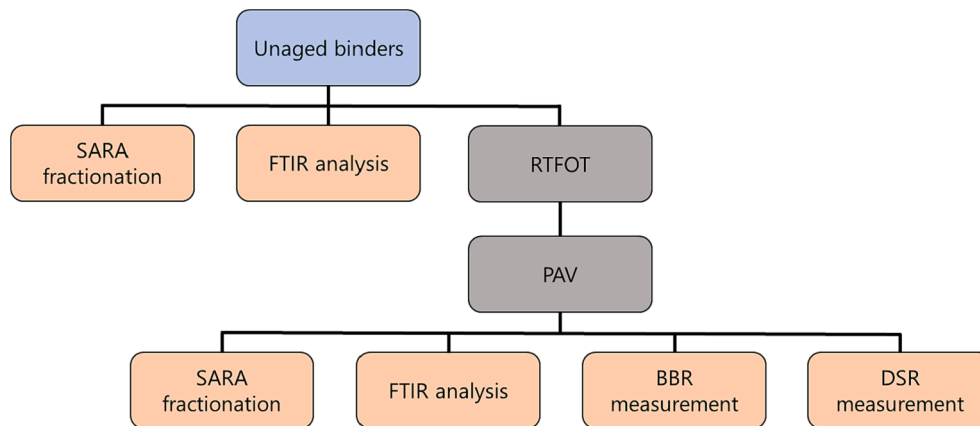

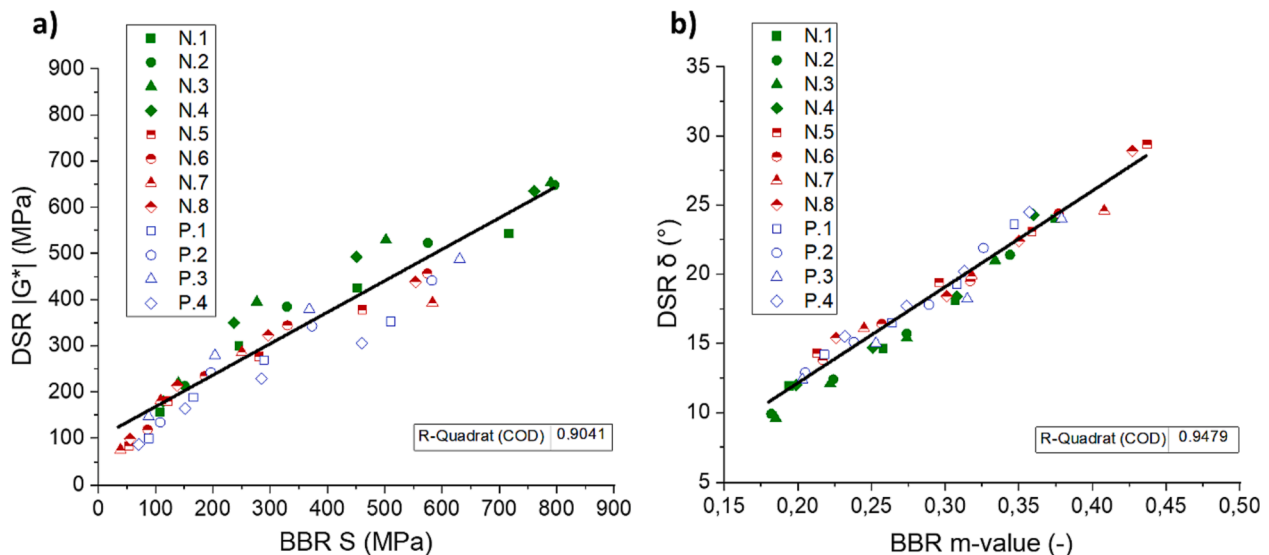**Fig. 2.** Flowchart of the performed aging and analysis methods.

Fig. 3. Correlation between DSR and BBR results at a DSR test frequency of 0.03183 Hz; a) complex modulus |G*| vs stiffness S and b) phase angle δ vs creep rate m-value.
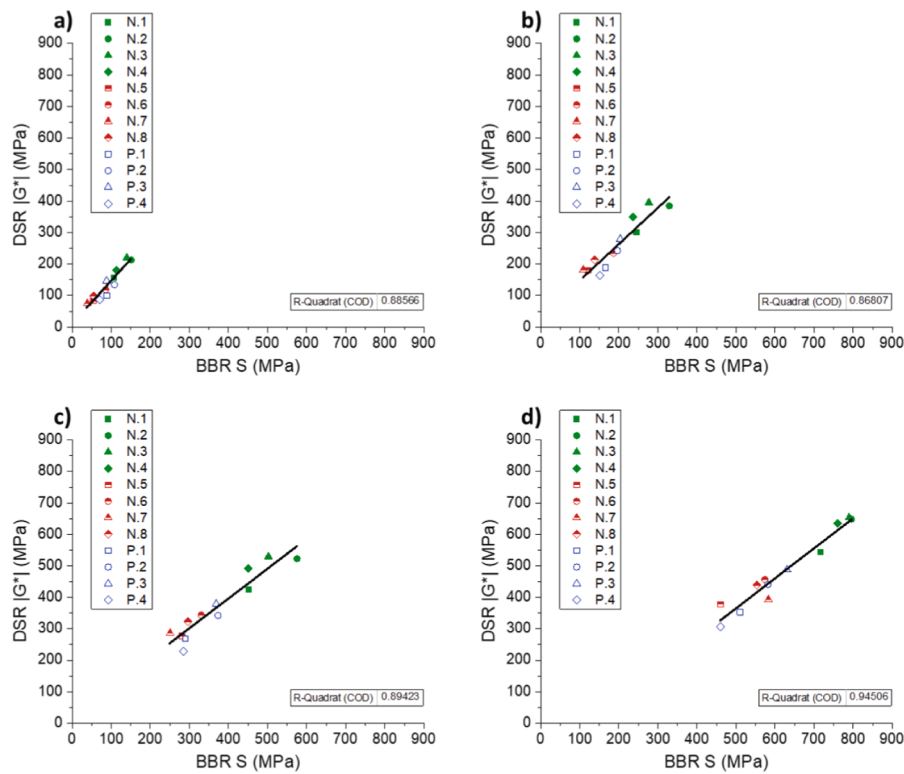
Fig. 4. Correlation between DSR complex modulus |G*| and BBR stiffness S; a) at −12 °C, b) at −18 °C, c) at −24 °C and d) at −30 °C.

impact of the differences in chemical composition and the polymer modification on the response to stress is not yet that pronounced. The fitted linear regression at this temperature shows an R^2 of 0.89, indicating an already rather high level of correlation between the data points. For the measurement results at −18 °C plotted in Fig. 4b an increasing maximum difference of 231 MPa for |G*| and of 168 MPa for S can be observed. The R^2 is with 0.87 the lowest for all four graphs, however the degree of linear correlation is still satisfactory. Moving on to a test temperature of −24 °C in Fig. 4c the R^2 is slightly increasing to 0.89 and also the span of the observed measurement results is broadening with a maximum difference of 300 MPa for |G*| and 325 MPa for S. At −24 °C the higher rigidity of the harder binders N.1 to N.4 is now

clearly represented by the large gap to the lower stiffnesses observed by the softer binders N.5 to N.8. Also, the polymer modification shows its significant benefit at this temperature, resulting in still rather low stiffnesses for the binders P.1 to P.4. This trend is confirmed in Fig. 4d for a testing temperature of −30 °C, where the maximum difference for |G*| and S is at 348 MPa and 335 MPa, respectively. Although, the range of the observed measurement results is the greatest at −30 °C, also the highest R^2 of 0.95 is presented at this temperature, indicating that the linear correlation between the DSR and BBR devices is more pronounced at lower temperatures.

Another parameter that might impact the correlation between DSR and BBR measurements is the test frequency of the DSR device.
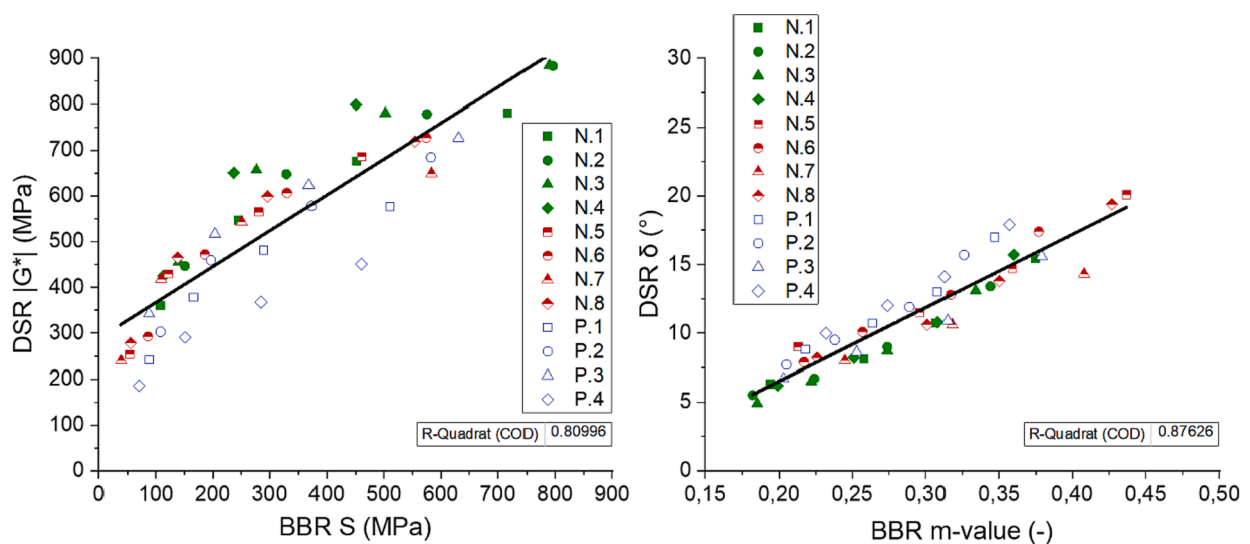

Fig. 5. Correlation between DSR and BBR results at a DSR test frequency of 1.592 Hz; a) complex modulus |G*| vs. stiffness S and b) phase angle δ vs. creep rate m-value.

Therefore, in Fig. 5 |G*| and δ are used at an applied test frequency of 1.592 Hz as opposed to 0.03183 Hz in Fig. 3. It can be seen that by correlating the two measurement devices at a frequency of 1.592 Hz the R^2 for |G*| vs S decreases from 0.90 to 0.81 and the R^2 for δ vs m-value decreases from 0.95 to 0.87. This strongly indicates, that the degree of linear correlation is dependent on the test frequency, at which the DSR measurements are performed. Furthermore, it is apparent that with this specific sample set a frequency of 0.03183 Hz is more suitable for the comparison of the two measurement devices, than a test frequency of 1.592.

3.2. Determination of the continuous low-temperature PG

For the determination of the continuous low-temperature PG based on BBR measurements standardized cut-off values are defined: 300 MPa for the stiffness S and 0.3 for the m-value [28]. The continuous low PG is then calculated following Equation (3) according to [29].

$$T_C = T_1 + \{\log_{10}(P_S) - \log_{10}(P_1)\} * \frac{T_2 - T_1}{\{\log_{10}(P_2) - \log_{10}(P_1)\}} - 10°C \quad (3)$$

T_C = continuous grading temperature for the specification requirement in question, °C.

T_1, T_2 = test temperatures, °C.

P_S = specification requirement for property in question.

P_1, P_2 = test result for specification property in question at T_1 and T_2, respectively.

For the determination of the continuous low-temperature PG based on DSR measurements, cut-off values had to be defined. The proposed cut-off values by Komaragiri et al. [19] did lead to rather large discrepancies when comparing the resulting low-temperature PG based on BBR and DSR measurements. Therefore, different cut-off values, which led to a better correlation, were chosen: 350 MPa was selected for the complex modulus |G*| and 18° for the phase angle δ. The continuous low PG was then calculated by plotting the respective measuring temperature against the complex modulus |G*| or the phase angle δ, generating a linear function and inserting the previously mentioned cut-off value.

In Fig. 6 the comparison of the continuous low PG based on DSR and BBR measurements can be seen, whereby in Fig. 6a BBR S and DSR |G*| and in Fig. 6b BBR m-value and DSR δ were used. Again, a distinct linear correlation between the two parameters is visible, whereby the twelve investigated binders divide up into the three grades PG −34, PG −28 and PG −22. In Fig. 6a the polymer-modified binders in blue show either a PG of −34 or −28 and are assigned the same grade by both methods. The soft binders with the color red are also either located in the PG −34 or −28 and for three of the four samples the grading based on BBR and based on DSR was the same. For the hard binders in green, PG −28 and

−22 apply and again three out of four binders show a matching PG, resulting in two out of twelve mismatched binder samples in total. When looking at the graph in Fig. 6b a similar picture can be seen. However, the polymer-modified binders in blue are now assigned to PG −28 and −22, indicating a significant discrepancy between S and m-value regarding BBR and |G*| and phase angle regarding DSR measurements. The other two groups of binders did not show different results and are still located in PG −28 and −22. Moreover, when using BBR m-value and DSR δ for PG grading, only one soft binder was mismatched. These results demonstrate the potential of the DSR device to properly characterize the low-temperature behavior of unmodified and polymer-modified bitumens by directly using |G*| or δ without any mathematical conversion. As of now the exact cut-off values seem to be influenced by the equipment in use, but a standardization should be possible by expanding the sample size and comparing different rheometers.

3.3. Correlation between continuous low-temperature PG and chemical properties

An important aspect of this study was to investigate the connection between the mechanical low-temperature performance of bitumen and their chemical composition. Therefore, ATR-FTIR spectroscopy and SARA fractionation was performed on all unaged and RTFOT + PAV aged binders, to gain information about the amount of incorporated oxygen and the changes in the polarity gradient of the investigated sample. In Fig. 7, the continuous low-temperature PG based on stiffness or creep rate (the respective higher temperature was chosen) and several chemical properties are juxtaposed: In the graphs a, c and e the unaged samples and in the graphs b, d and f the RTFOT + PAV aged samples are located. In the first row, the AI_{FTIR} is plotted on the x-axis for an estimation of the amount of incorporated oxygen. In the second row, the asphaltene content is plotted on the x-axis. Since the asphaltene fraction significantly increases when the material undergoes oxidation, information about the amount of aging from a polarity point of view can be gathered from these graphs. In the last row, the ratio of different SARA fractions calculated according to Equation (4) [30] is plotted on the x-axis. This parameter is defined as the polarity index, which puts the amount of saturates and aromatics and the amount of resins and asphaltenes into relation. The ratio of the components with lower polarity are compared to the components with a higher polarity, giving information about the amount of high polar structures in the material.

$$\text{Polarity Index} = \frac{(\text{Resins} + \text{Asphaltenes})}{(\text{Saturates} + \text{Aromatics})} \quad (4)$$

When looking at the investigated chemical properties in the unaged and in the RTFOT + PAV aged state a general increase is visible. The AI_{FTIR} increased on average by 0.11, the asphaltene content by 6.3 % and the polarity index by 0.27. This could be explained by the fact, that a higher AI_{FTIR} indicates a higher amount of incorporated oxygen and
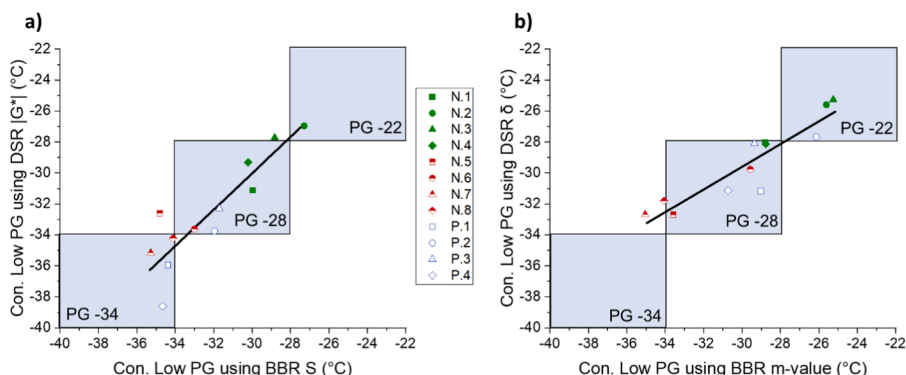
Fig. 6. a) Determination of the continuous low PG using BBR S vs. DSR|G*| and b) BBR m-value vs. DSR δ.
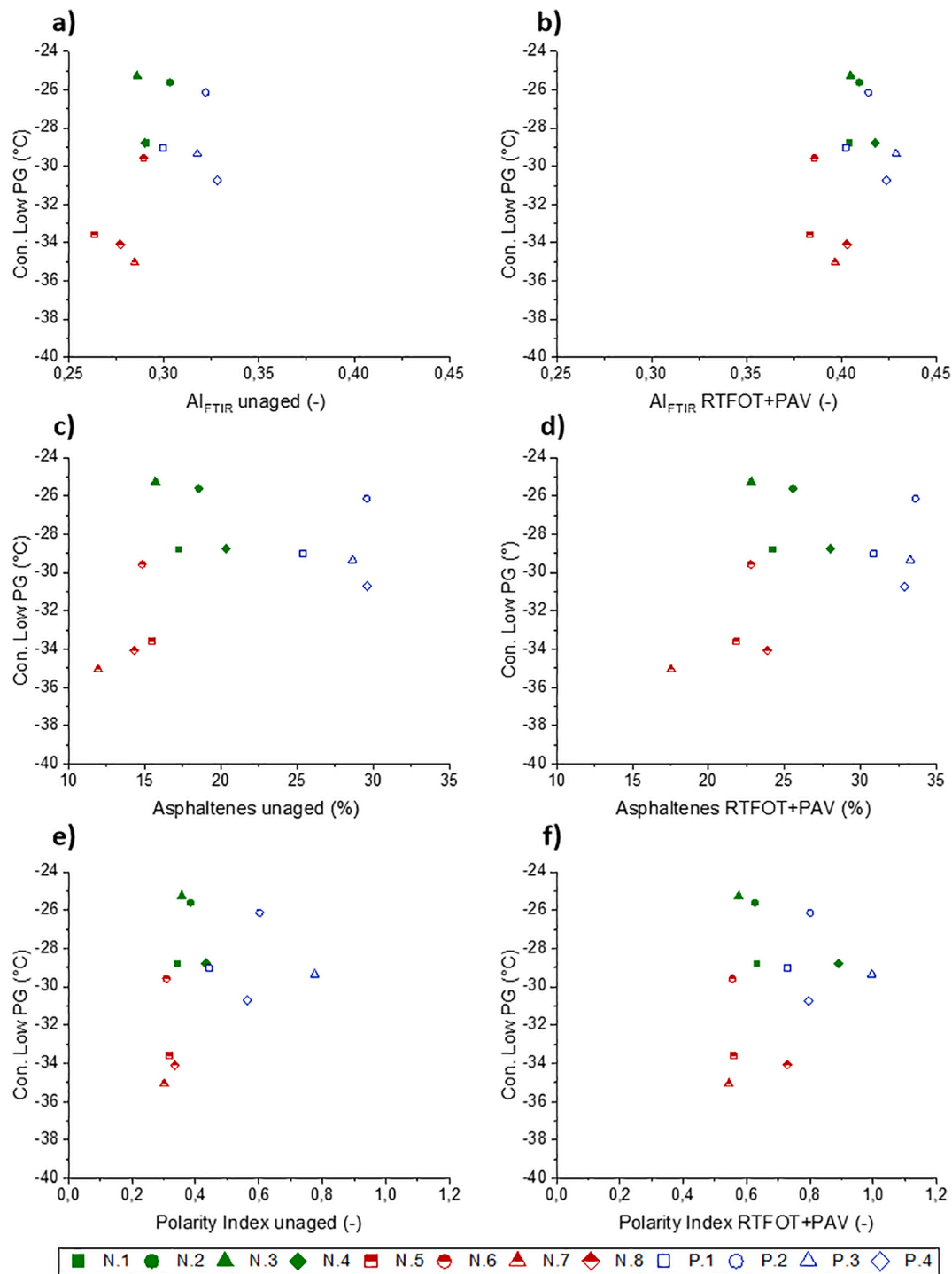
Fig. 7. Comparison of continuous low PG and several chemical properties (AI_{FTIR}, asphaltene content and polarity index).

therefore a higher amount of polar chemical compounds in the material. High polar chemical structures can be usually found in the asphaltene fractions, which results in a high asphaltene content and also in a high polarity index. Moreover, a correlation with the continuous low PG can be seen, whereby a higher continuous low PG corresponds to a higher value for the respective chemical property. This link is visible for all three parameters, however the AI_{FTIR} shows the most coherent and pronounced relation. The increasing low-temperature PG could be caused by highly polar chemical structures interacting more strongly with each other and forming a network in the material, which in turn increases the viscosity and therefore impairs the ability to relax induced

stresses. The possibility of obtaining information about the low-temperature behavior of bitumens by ATR-FTIR spectroscopy allows for a fast and simple characterization of samples with a short sample preparation and data analysis times. Possible applications could be the broad classification of a sample group or the obtainment of preliminary information about different binders.

Another point, that is visible when looking at the graphs with the results for the unaged binders, is a slight division into the three different binder groups (soft, hard and polymer-modified). However, this division becomes less distinct when looking at the results for the RTFOT + PAV aged state. It can be seen that the four investigated polymer-modified

binders already have a higher AI_{FTIR}, asphaltene content and polarity index in the unaged state, which results in a position more to the right compared to the non-modified binder groups. The AI_{FTIR}, asphaltene content and polarity index increased on average only by 30 % for the polymer-modified binders and by 60 % for the non-modified binders. The PmB group showed less aging during RTFOT + PAV, leading to a decrease in the gap to the other samples and a more even mixing of the different data points especially when looking at the AI_{FTIR} and the polarity index. Although, the differentiation between the soft and the hard binder group is mainly based on the different low PG grades, a minor shift to the right can be seen when looking at the chemical properties on the x-axis for the hard binders. This indicates, that binders with a lower needle penetration and a higher softening point also show slightly higher values for the AI_{FTIR}, asphaltene content and polarity index in an unaged and RTFOT + PAV aged state.

3.4. Correlation between ΔT_c and chemical properties

Another important parameter that has been investigated regarding the low-temperature properties of bituminous binders is the difference in the low-temperature PG limiting temperatures based on BBR S and m-value, referred to as ΔT_c. It gives information about the general aging behavior and relaxation properties of the investigated material. In Fig. 8, the correlation between ΔT_c and the previously displayed chemical properties of the binders is shown, whereby ΔAI_{FTIR}, ΔAsphaltenes, ΔPolarity Index, and ΔColloidal Instability Index (CII) are plotted on the x-axis, respectively. These indicators present the change that the material undergoes from the unaged to the RTFOT + PAV aged state. Since the AI_{FTIR} is mainly calculated with the area of the carbonyl and the

sulfoxide band, ΔAI_{FTIR} indicates the increase of these chemical structures during the long-term aging process. Additionally, a slight percentage of the integration values of the carbonyls and sulfoxides originates from the intensity increase observed in the fingerprint region upon aging, as the FTIR integration was performed using a full base line integration method. ΔAsphaltenes represents the change of the asphaltene content and ΔPolarity Index the change of the polarity gradient in the binder sample. The CII is an indicator for the stability of a bituminous material and can be calculated according to Equation (5) [31].

$$CII = \frac{Saturates + Asphaltenes}{Aromatics + Resins} \tag{5}$$

From a mechanical point of view, it is possible that larger values for ΔAI_{FTIR}, ΔAsphaltenes, ΔPolarity Index are correlated to a stronger increase in the stiffness or also a stonger decrease in the ability to dissipate stresses. A larger value for ΔCII indicates a strong increase in asphaltenes and/or saturate and a decrease of the stability of the binder.

ΔT_c is plotted on the y-axis. Generally, it can be seen, that the polymer-modified bitumens exhibit the most negative values for ΔT_c, followed by the hard and then the soft unmodified binders. This effect has been observed in the past, whereby the addition of styrene–butadienestyrene (SBS) to an unmodified binder led to an increasingly negative ΔT_c, which not necessarily goes along with poor stress relaxation properties [21]. A characterization of polymer-modified binders with ΔT_c is therefore still possible, however the comparison to unmodified samples or the missing knowledge of the polymer modification could pose difficulties.

In Fig. 8a, it can be seen, that there is an indirect proportional correlation between ΔT_c and ΔAI_{FTIR}, indicating that a greater difference
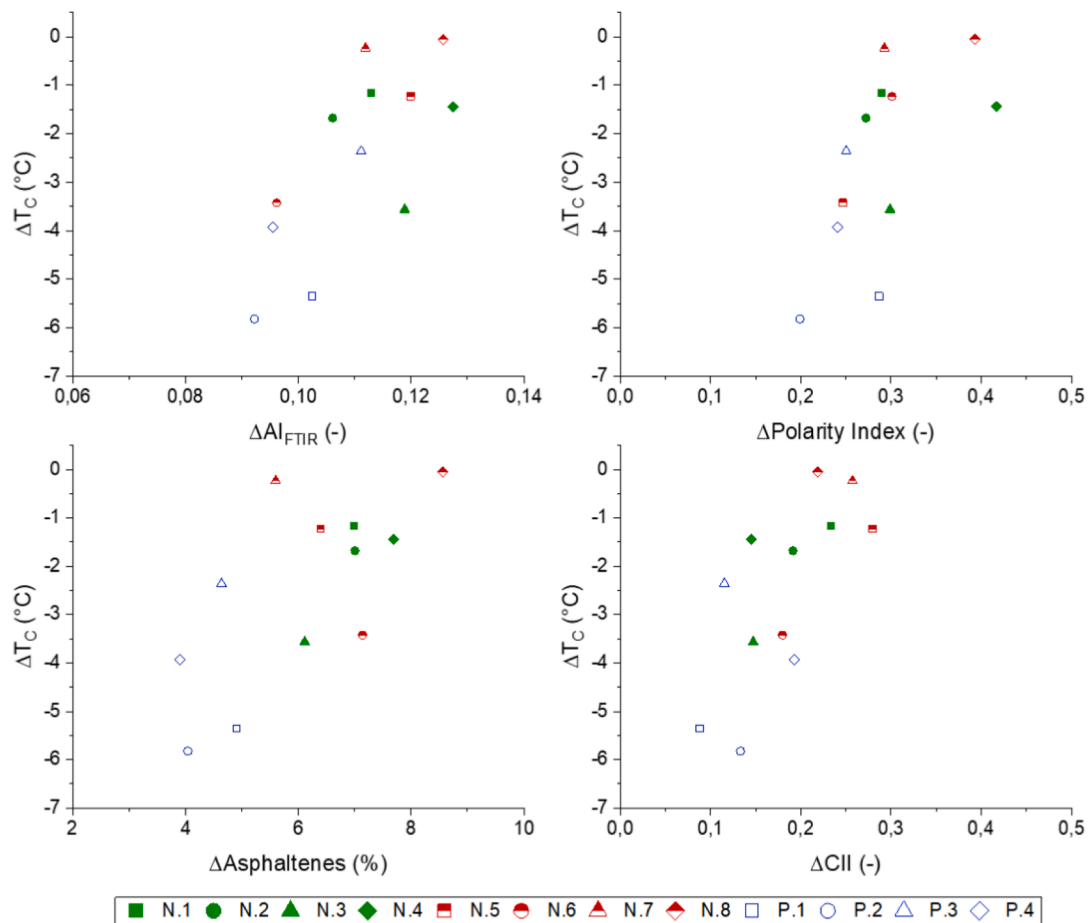

Fig. 8. Comparison of ΔT_c and several chemical properties (AI_{FTIR}, asphaltene content, polarity index and colloidal instability index).

between the PG limiting temperatures corresponds to less aging taking place during RTFOT + PAV. The overall highest value for ΔAI_{FTIR} and the corresponding lowest magnitude for ΔT_c could be observed for the soft binders depicted in red. A similar relationship is apparent for the correlation between ΔT_c and $\Delta Asphaltenes$, which can be seen Fig. 8c. The results indicate that a stronger change in the asphaltene content of the material goes along with a more distinct difference in the low PG limiting temperatures. This again states that the investigated bitumen with higher magnitudes for ΔT_c exhibit less aging during RTFOT + PAV. This trend is also confirmed when looking at the correlation between ΔT_c and $\Delta Polarity Index$ in Fig. 8b and at the correlation between ΔT_c and ΔCII in Fig. 8d. In both of these graphs, a ratio between the different SARA fractions of the investigated binders is plotted on the x-axis, whereby the polarity index gives information about the amount of high polar compounds in the material and the CII gives information about the polarity gradient in the material and the mixture stability. The same overall trend is visible, showing a decreasing $\Delta Polarity Index$ and ΔCII with an increasing ΔT_c, again indicating that less aging took place during RTFOT + PAV.

3.5. Correlation between different chemical properties

In the previous sections, the links of the mechanical properties continuous low-temperature PG and ΔT_C to the chemical properties ΔAI_{FTIR}, $\Delta Asphaltenes$, $\Delta Polarity Index$, and ΔCII were discussed in detail. These parameters were obtained by FTIR spectroscopy and SARA fractionation. Although both of these methods provide information about the chemical composition of the investigated sample, the principle of analysis is fundamentally different. This raises the question, whether a correlation between results from these methods exists. In Fig. 9 the relationship between the AI_{FTIR} on the x-axis and the polarity index on the y-axis can be seen, whereby the unaged state, the RTFOT + PAV aged state and the difference of these two aging states are presented successively. A slight classification of the data points into the different binder groups "soft" depicted in red, "hard" in green and polymer-modified" in blue is visible.

The investigated polymer-modified bitumen show an already higher amount of resins and asphaltenes and a higher amount of incorporated oxygen in the unaged state. However, the gap to the non-modified binders is smaller after RTFOT + PAV aging, which underlines the fact, that the modified binders undergo less change in these chemical properties with the aging process. Moreover, in all three graphs, a linear direct proportional correlation between AI_{FTIR} and polarity index can be observed, indicating that a higher AI_{FTIR} corresponds to a higher polarity index. This can be explained by the fact, that the AI_{FTIR} represents the amount of incorporated oxygen and this value affects the polarity of the sample. The formation of high polar structures in the material can be a direct result of the chemical reaction and incorporation of oxygen into the sample, which influences both the polarity index and the AI_{FTIR}. This link is apparent for the unaged and for the RTFOT + PAV aged state, whereby both investigated parameters show higher values after aging. As already mentioned, the change of the two properties depicted in Fig. 9c shows a direct proportional correlation, affirming the possibility, that a change due to aging in the SARA composition of the investigated binder sample may be detected using FTIR spectroscopy.
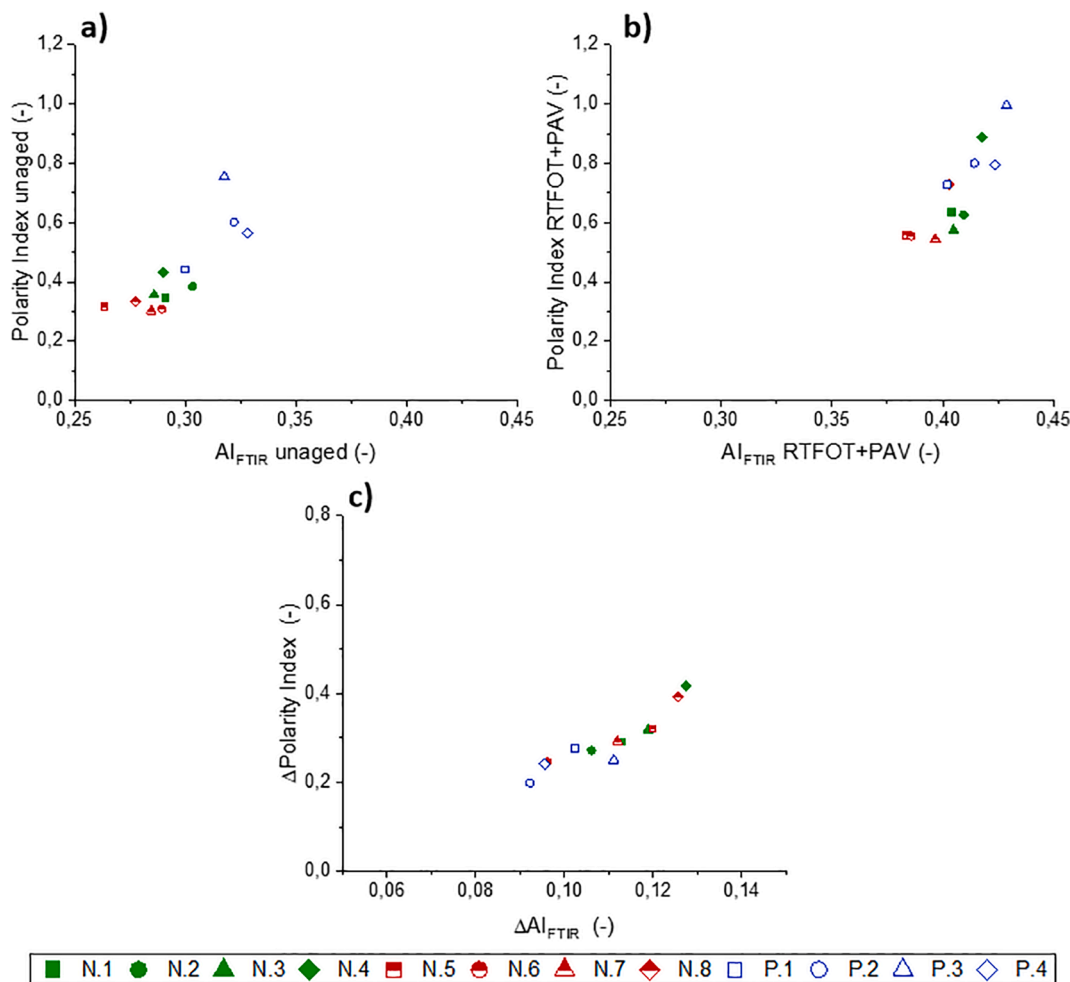

Fig. 9. Comparison of the AI_{FTIR} and the polarity index.

4. Conclusions

In this study, DSR measurements were directly correlated to BBR results and subsequently used for the characterization of the low-temperature properties of 12 investigated bituminous binders. Furthermore, FTIR analysis and SARA fractionation have been performed to determine the degree of aging via indices such as AI_{FTIR}, asphaltene content, polarity index and CII. From the performed measurements the following conclusions can be drawn:

1. The results show that the BBR stiffness and DSR complex modulus, as well as the BBR m-value and DSR phase angle exhibit a linear correlation with high coefficients of determination. This verifies the existence of a fundamental link between the two devices, which proves the general possibility of directly interchanging the methods without the need for performing linear visco-elastic interconversions.

2. For the determination of the low-temperature PG, cut-off values were set at 350 MPa for the complex modulus and at 18° for the phase angle. The use of DSR $|G^*|$ allowed for 10 and the use of DSR δ for 11 out of 12 matching performance grades, respectively. This demonstrates that it is possible to assign the proper low-temperature PG with the DSR by using only very small quantities of the material.

3. The investigated samples with a lower possible application temperature also showed lower values for the AI_{FTIR}, the asphaltene content and the polarity index. Furthermore, an indirect proportional correlation between ΔT_c and ΔAI_{FTIR}, $\Delta Asphaltenes$, $\Delta Polarity$ Index and ΔCII could be observed. This illustrates the potential of FTIR spectroscopy and SARA fractionation being able to give information about the low-temperature behavior of bitumen. Additionally, a linear correlation between the AI_{FTIR} and the polarity index could be observed, which can be explained by the fact that both methods give information of the amount of incorporated oxygen to some degree.

Due to the limited sample size at this point, the observed tendencies do not offer final proof of these correlations, but they show once more the potential of fast and easy-to-use chemical analysis methods in bitumen assessment. The results provide another step into the direction of combining chemical and mechanical analysis methods to gather relevant information about the investigated material in a short period of time.

CRediT authorship contribution statement

Kristina Hofer: Investigation, Conceptualization, Writing – original draft. **Johannes Mirwald:** Conceptualization, Supervision, Writing – review & editing. **Amit Bhasin:** Conceptualization, Writing – review & editing. **Bernhard Hofko:** Project administration, Conceptualization, Supervision, Resources, Writing – review & editing.

Declaration of Competing Interest

The authors declare that they have no known competing financial interests or personal relationships that could have appeared to influence the work reported in this paper.

Data availability

Data will be made available on request.

Acknowledgments

References

[1] J.C. Petersen, A review of the fundamentals of asphalt oxidation: chemical, physicochemical, physical property, and durability relationships, Transport. Res. Circular (2009) (E-C140).

[2] D. Lesueur, The colloidal structure of bitumen: Consequences on the rheology and on the mechanisms of bitumen modification, Adv. Colloid Interface Sci. 145 (1) (2009) 42–82.

[3] U. Isacsson, H. Zeng, Relationships between bitumen chemistry and low temperature behaviour of asphalt, Construct. Build. Mater. 11 (2) (1997) 83–91.

[4] U. Isacsson, H. Zeng, Cracking of asphalt at low temperature as related to bitumen rheology, J. Mater. Sci. 33 (8) (1998) 2165–2170.

[5] Jung, D. and T.S. Vinson, *Low-temperature cracking: binder validation.* 1994.

[6] H.U. Bahia, D.A. Anderson, D.W. Christensen, The bending beam rheometer; a simple device for measuring low-temperature rheology of asphalt binders (with discussion), J. Assoc. Asphalt Paving Technol. 61 (1992).

[7] C. Sui, et al., New technique for measuring low-temperature properties of asphalt binders with small amounts of material, Transport. Res. ch Rec. J. Transport. Res. Board 2179 (2010) 23–28.

[8] M. Farrar, et al., Determining the low-temperature rheological properties of asphalt binder using a dynamic shear rheometer (DSR), Report 4FP 8 (2015) 20.

[9] J. Büchner, et al., On low temperature binder testing using DSR 4 mm geometry, Mater. Struct. 52 (6) (2019) 113.

[10] J. Gražulytè, et al., Analysis of 4-mm DSR tests: calibration, sample preparation, and evaluation of repeatability and reproducibility, Road Mater. Pav. Design 22 (3) (2021) 557–571.

[11] J. Büchner, et al., Interlaboratory study on low temperature asphalt binder testing using Dynamic Shear Rheometer with 4 mm diameter parallel plate geometry, Road Mater. Pavement Design (2020) 1–17.

[12] van Heerden, J. and J. Muller. *Rheology of binder low temperature cracking: A comparative study of two different instruments employing different testing geometries.* in *Conference on Asphalt Pavements for Southern Africa (CAPSA15), 11th, 2015, Sun City, South Africa.* 2015.

[13] X. Lu, P. Uhlback, H. Soenen, Investigation of bitumen low temperature properties using a dynamic shear rheometer with 4mm parallel plates, Int. J. Pavement Res. Technol. 10 (1) (2017) 15–22.

[14] O.-V. Laukkanen, et al., Low-temperature rheological and morphological characterization of SBS modified bitumen, Constr. Build. Mater. 179 (2018) 348–359.

[15] M. Marasteanu, D. Anderson, Improved model for bitumen rheological characterization. Eurobitume Workshop On Performance Related Properties For Bituminous Binders, European Bitumen Association Brussels, Belgium, 1999.

[16] Oshone, M.T., *Performance based evaluation of cracking in asphalt concrete using viscoelastic and fracture properties.* 2018, University of New Hampshire.

[17] C. Sui, et al., New low-temperature performance-grading method: Using 4-mm parallel plates on a dynamic shear rheometer, Transp. Res. Rec. 2207 (1) (2011) 43–48.

[18] R. Hajj, et al., Considerations for using the 4 mm plate geometry in the dynamic shear rheometer for low temperature evaluation of asphalt binders, Transp. Res. Rec. 2673 (11) (2019) 649–659.

[19] S. Komaragiri, et al., Using the dynamic shear rheometer for low-temperature grading of asphalt binders, J. Test. Eval. 50 (3) (2022).

[20] Committee, A.I.T.A., State-of-the-knowledge: use of the delta Tc parameter to characterize asphalt binder behavior. Asphalt Institute Technical Document, 2019.

[21] Baumgardner, G., *Delta Tc Binder Specification Parameter [tech brief].* 2021.

[22] R.M. Anderson, et al., Evaluation of the relationship between asphalt binder properties and non-load related cracking, J. Assoc. Asphalt Paving Technol. 80 (2011).

[23] ASTM, *ASTM D2872-21: Standard Test Method for Effect of Heat and Air on a Moving Film of Asphalt (Rolling Thin-Film Oven Test).* 2021, ASTM International. p. 6.

[24] ASTM, *ASTM D6521-19a: Standard Practice for Accelerated Aging of Asphalt Binder Using a Pressurized Aging Vessel (PAV).* 2019, ASTM International. p. 7.

[25] ASTM, *ASTM D6648-08(2016): Standard Test Method for Determining the Flexural Creep Stiffness of Asphalt Binder Using the Bending Beam Rheometer (BBR).* 2016, ASTM International. p. 15.

[26] J. Mirwald, D. Nura, B. Hofko, Recommendations for handling bitumen prior to FTIR spectroscopy, Mater. Struct. 55 (2) (2022) 26.

[27] N. Sakib, A. Bhasin, Measuring polarity-based distributions (SARA) of bitumen using simplified chromatographic techniques, Int. J. Pavement Eng. 20 (12) (2019) 1371–1384.

[28] ASTM, ASTM D6373-21a: Standard Specification for Performance-Graded Asphalt Binder. 2021, ASTM International. p. 5.

[29] ASTM, *ASTM D7643-16: Standard Practice for Determining the Continuous Grading Temperatures and Continuous Grades for PG Graded Asphalt Binders1.* 2016, ASTM International. p. 5.

[30] J. Mirwald, et al., Understanding bitumen ageing by investigation of its polarity fractions, Constr. Build. Mater. 250 (2020).

[31] S. Asomaning, A.P.W., Petroleum stability and heteroatom species effects in fouling of heat exchangers by asphaltenes, Heat Transfer Eng. 21 (3) (2000) 10–16.